DOI: 10.1002/zaac.201300569

# Mitochondria targeting Photocytotoxic Oxidovanadium(IV) Complexes of Curcumin and (Acridinyl)dipyridophenazine in Visible Light

**Samya Banerjee,[a] Puja Prasad,[a] Imran Khan,[b] Akhtar Hussain,[a] Paturu Kondaiah,*[b] and Akhil R. Chakravarty*[a]**

*Dedicated to Professor C. N. R. Rao on the Occasion of His 80th Birthday*

**Keywords:** Curcumin; Vanadium; Photocytotoxicity; Apoptosis; Cytosolic localization

**Abstract**. Oxidovanadium(IV) complexes, [VO(acac)(L)Cl] (**1**), [VO(cur)(L)Cl] (**2**), and [VO(scur)(L)Cl] (**3**) {acac = acetylacetonate, cur = curcumin monoanion, scur = diglucosylcurcumin monoanion, L = 11-(9-acridinyl)dipyrido[3,2-a:2',3'-c]phenazine (acdppz)}, were prepared and characterized. The complexes are non-electrolytic in DMF and 1:1 electrolytic in aqueous DMF. The one-electron paramagnetic complexes showed a d-d band near 725 nm in aqueous DMF and green emission near 520 nm in aqueous DMSO. The complexes exhibited an irreversible $V^{IV}/V^{III}$ redox response near –0.85 V versus SCE in aqueous DMF. The complexes showed good binding strengths to calf thymus DNA ($K_b$: $3.1 \times 10^5$–$9.6 \times 10^5$ $M^{-1}$) and efficient pUC19 DNA photocleavage activity in red light of 705 and 785 nm by singlet oxygen ($^1O_2$) pathway. Complexes **1** and **2** exhibited significant photocytotoxicity ($IC_{50}$: 0.1–1.0 μM) in visible light (400–700 nm) with low dark toxicity ($IC_{50}$: >20 μM) in HeLa and HaCaT cells. Complex **3** was cytotoxic in both light and dark. DNA ladder formation experiments indicated cell death via apoptotic pathway. Confocal microscopy done with **1** and **2** revealed primarily cytosolic localization of the complexes with significant presence of the complex in the mitochondria as evidenced from the imaging data using mitotracker red.

## Introduction

Curcumin, the major ingredient of turmeric, is used as traditional herbal medicine to treat infections, bite, burns, and skin diseases.[1] It is known to show a wide range of biological activities.[2] It exhibits anticancer activity due to its ability to induce apoptosis in cancer cells without any significant cytotoxic effects on normal cells.[3] Curcumin is reported to interfere with the activity of the transcription factor NF-κB which is a protein complex involved in the transcription of DNA and known to enhance the activity of the tumor suppressor protein p53.[2,4,5] However, clinical application of curcumin [Hcur = 1,7-bis(4-hydroxy-3-methoxyphenyl)-1,6-hepta-diene-3,5-dione] is limited due to its poor bioavailability and pharmacokinetic profile resulting from its hydrolytic instability under physiological conditions.[6] This is largely attributed to the presence of a reactive β-diketone moiety in its structure. Binding of this moiety to an oxophilic metal ion is reported to increase the hydrolytic stability and bioavailability of curcumin.[7,8] Although several studies on the anticancer properties of curcumin and its metal complexes are reported, their utility as photodynamic therapy (PDT) agents remains virtually unexplored.[3,6,9]

The motivation to explore the medicinal chemistry of curcumin in light has led us to design and synthesize new ternary oxidovanadium(IV) complexes of curcumin and its glycosylated derivative showing photo-induced cytotoxicity in visible light in cancer cells. Vanadium is a biocompatible metal ion and its complexes have earlier been used as insulin mimetics and antitumor agents.[10,11] Bleomycin oxidovanadium(IV) and $[VO(phen)(H_2O)_2]^{2+}$ are known to show chemical nuclease activity in the presence of $H_2O_2$.[12,13] There are few reports on oxidovanadium(V) and peroxidovanadium(V) complexes cleaving DNA on photo-activation using UV light source, which is undesirable in photodynamic therapy (PDT) due low tissue penetration of UV light.[14,15] In contrast, oxidovanadium(IV) complexes displaying a low energy d-d absorption band in the red light window are suitable for PDT considering greater tissue penetration of red light.[16,17] Besides, the green emission of 11-(9-acridinyl)dipyrido[3,2-a:2′,3′-c]-phenazine (acdppz) and curcumin (Hcur) complexes designed in this work could be utilized to study the cellular uptake and localization of the complexes in cancer cells by confocal fluorescence microscopy. We have designed and prepared new ternary oxidovanadium(IV) complexes based on our dual strat-

* Prof. Dr. P. Kondaiah
E-Mail: paturu@mrdg.iisc.ernet.in
* Prof. Dr. A. R. Chakravarty
Fax: +91-80-23600683
E-Mail: arc@ipc.iisc.ernet.in
[a] Department of Inorganic and Physical Chemistry
Indian Institute of Science
Bangalore-560012, India
[b] Department of Molecular Reproduction,
Development and Genetics
Indian Institute of Science
Bangalore 560012, India

Supporting information for this article is available on the WWW under **http://dx.doi.org/10.1002/zaac.201300569** or from the author.



  

egy of combining imaging with therapy. Glycosylation of curcumin is done to increase the aqueous solubility of the resulting complexes.[18] In addition, appending a glucose moiety has proved to be successful in augmenting the cellular uptake of the compounds into the cancer cells having high density of glucose receptors compared to that in the normal cells.[19] We have chosen acdppz ligand in the ternary structure for its green emissive and strong DNA intercalating property. The increased planarity and conjugation in this ligand is expected to enhance the photocytotoxicity of the resulting complexes.[20]

Herein we present the synthesis, characterization, and visible light-induced photocytotoxicity of three new oxidovanadium(IV) complexes, [VO(acac)(L)Cl] (**1**), [VO(cur)(L)Cl] (**2**) and [VO(scur)(L)Cl] (**3**) {acac = acetylacetonate (in **1**), Hcur = curcumin (in **2**), Hscur = diglucosylcurcumin (in **3**), and L = 11-(9-acridinyl)dipyrido[3,2-a:2′,3′-c]phenazine (acdppz) (in **1**–**3**)} (Figure 1). Significant results of this study include remarkable photocytotoxicity of the complexes at nanomolar concentration in human cervical cancer cell line (HeLa) ($IC_{50}$: 0.3–1.0 μM) and human skin keratinocyte cell line (HaCaT) ($IC_{50}$: <0.4 μM) in visible light of 400–700 nm with low dark toxicity thus showing similar activity as the clinically approved PDT drug Photofrin®.[21] The cellular imaging studies showed desirable cytosolic uptake of the complexes (**1**, **2**) within 4 h of incubation, which compares well with that of Photofrin®. Observation of mitochondrial localization of the complexes is significant considering that the pathway of apoptosis largely involves the mitochondria as is known for the PDT drug Photofrin®.[22–25] The mitochondria targeting PDT agents could overcome any resistance mechanism that are involved for conventional chemotherapeutic agents targeting the nuclear DNA. In addition, the present complexes show cellular damage in light generating singlet oxygen ($^1O_2$) as the reactive oxygen species (ROS) like Photofrin® as evidenced from the mechanistic data obtained from the plasmid DNA photocleavage experiments. Having many functional similarities with the PDT drug Photofrin®, complex **2** is unique in the chemistry of 3d metal-based PDT agents.[26]

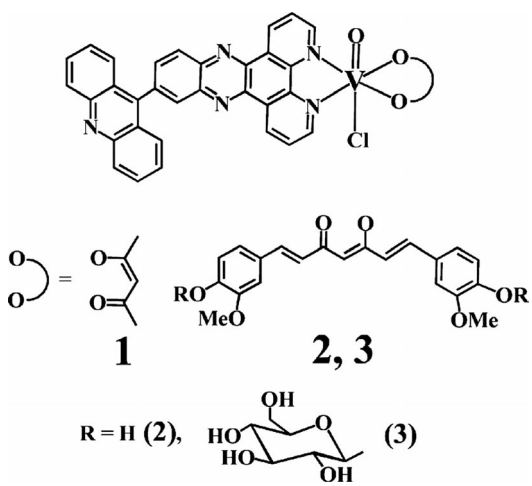


**Figure 1**. Schematic drawing of the complexes **1**–**3** and the ligands used.

## Results and Discussion

### *Synthesis and Characterization*

The complexes were prepared in good yield by treating vanadyl sulfate with barium chloride in aqueous ethanol (1:5 v/v water-ethanol) and the filtrate after removal of barium sulfate was subsequently reacted with acdppz base in chloroform-ethanol (2:3 v/v) and respective acetylacetone (Hacac), curcumin (Hcur), or glycosylated curcumin (Hscur) ligand in acetonitrile-ethanol mixture. The complexes were characterized from the analytical and physicochemical data (Table 1). The ESI-MS of the complexes showed essentially a single peak corresponding to the $[M - Cl]^+$ in MeOH. The complexes were found to be stable in the solution phase as five-coordinate species [VO(cur)(L)]Cl as evidenced from the mass spectroscopic data. The complexes gave molar conductance values of approx. 20 and approx. 95 $S{\cdot}m^2{\cdot}M^{-1}$ in pure DMF and 20% aqueous DMF, respectively, suggesting their non-electrolytic behavior in DMF and 1:1 electrolytic nature in aqueous medium due to dissociation of the chloride ligand.[27] The room temperature magnetic moment ($\mu_{eff}$) values of 1.6 $\mu_B$ implied one-electron paramagnetic nature of the $3d^1$-$V^{IV}$ complexes. The IR spectra of the complexes showed three bands centred around 1588, 1495, and 965 $cm^{-1}$ for the C=O, C=C (β-diketonate), and V=O stretching vibrations, respectively.[28] The strong intensity IR band at 1588 $cm^{-1}$ (C=O stretching) indicates bidentate coordination mode of the β-diketone (acac/cur/scur) ligand to the central metal atom. The complexes displayed a d–d band in the electronic spectra in the wavelength range of 717–729 nm in 20% DMF-water (Figure 2, Table 1). Complex **2** showed an intense curcumin-based visible band at 437 nm due to $\pi \rightarrow \pi^*$ transition with a shoulder at around 454 nm.[9] The

**Table 1.** Selected physicochemical data and ct-DNA binding parameters of the complexes **1**–**3**.

| Complex | IR /$cm^{-1}$ $\tilde{\nu}$(C=O) | $\tilde{\nu}$(V=O) | Electronic [a]: λmax /nm (ε /$dm^3{\cdot}M^{-1}{\cdot}cm^{-1}$) | $\lambda_f$ /nm ($\Phi_f$ [b]) | $\mu_{eff}$ [c] | $\Lambda_M$ [d] /$S{\cdot}m^2{\cdot}M^{-1}$ | $E_{pc}$ [e] /V | $K_b$ [f] /$M^{-1}$ | $\Delta T_m$ [g] /°C |
|---|---|---|---|---|---|---|---|---|---|
| **1** | 1591 | 965 | 717 (47) | 523(0.02) | 1.63 | 111 | –1.01 | $(3.1 \pm 0.2) \times 10^5$ | 5.1 |
| **2** | 1586 | 967 | 725 (51) | 520(0.03) | 1.65 | 92 | –0.84 | $(8.9 \pm 0.4) \times 10^5$ | 6.5 |
| **3** | 1589 | 962 | 729 (54) | 516(0.026) | 1.62 | 81 | –0.82 | $(9.6 \pm 0.1) \times 10^5$ | 7.4 |

a) Visible electronic spectral band in 20% DMF-water. b) Emission spectra and quantum yield of **1**–**3** in aqueous DMSO (1:20 v/v), $\lambda_{exi}$ (nm) = 390. c) Magnetic moment ($\mu_{eff}$) in μB obtained by NMR method at 298 K. d) $\Lambda_M$, molar conductivity in 20% aqueous DMF at 25 °C. The complexes are non-electrolytic in pure DMF. e) Cathodic peak potential in 20% aq. DMF-0.1 M TBAP at 50 $mV{\cdot}s^{-1}$ scan rate. f) Equilibrium ct-DNA binding constant from the UV/Vis absorption experiments. g) Change in the ct-DNA melting temperature.

  

$\pi \rightarrow \pi^*$ band for the diglucosylcurcumin complex **3** was observed at 426 nm. The acdppz ligand in the complexes showed two additional bands near 362 nm and 390 nm assignable to the $\pi$–$\pi^*$ transition of the dppz and acridine chromophores.[20,29]

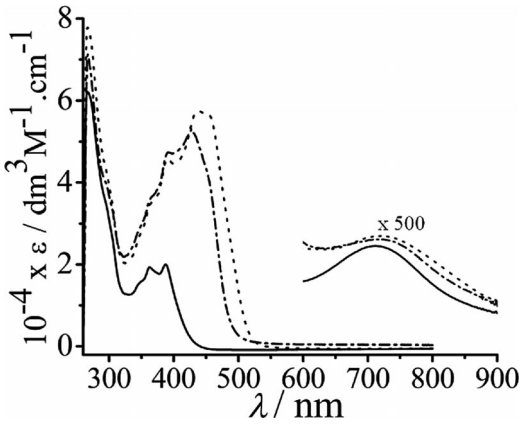


**Figure 2.** Electronic absorption spectra of complexes **1** (—), **2** (···) and **3** (-·-) in 20% aqueous DMF.

The complexes showed an emission band near 520 nm in aqueous DMSO (1:20 v/v) giving fluorescence quantum yield ($\phi$) values in the range of 0.02–0.03 (Figure 3, Table 1). The curcumin ligand alone gave a $\phi$ value of 0.042 under similar experimental conditions. The curcumin ligand-based fluorescence is thus retained in the oxidovanadium(IV) complexes and this allowed us to study the cellular uptake and localization of the complexes by confocal imaging. Cyclic voltammetry of the complexes showed a reduction process assignable to the $V^{IV}$-$V^{III}$ redox couple near –0.85 V versus S.C.E. in 20% DMF-$H_2O$ with 0.1 M [$n$Bu$_4$N](ClO$_4$) (TBAP) as the supporting electrolyte. The complexes did not show any oxidative response. The redox stability of the $VO^{2+}$ moiety over a wide potential window could reduce the dark toxicity of the complexes.

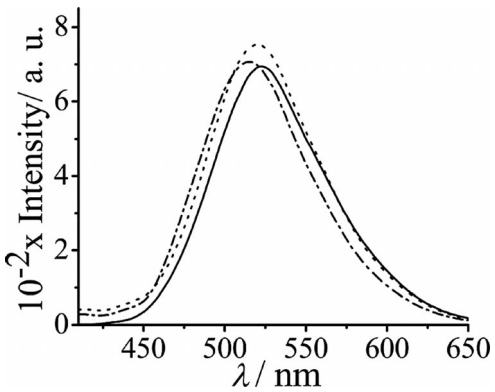


**Figure 3.** Emission spectra of **1**–**3** in aqueous DMSO (1:20 v/v) ($\lambda_{excitation}$ = 390 nm).

### *Computational Study*

To rationalize the photophysical properties of the complexes, computational studies were performed for complexes **2** and **3** using B3LYP/LANL2DZ level of DFT.[30] The energy optimized structures of the complexes showed an oxidovanadium(IV) moiety bonded to the chelating N,N-donor acdppz, O,O-donor monoanionic cur/scur ligand, and a chloride anion giving a $V^{IV}N_2O_3Cl$ core in a distorted octahedral arrangement. The axial V=O bond length is 1.61 Å, whereas the other V–O bond lengths are 1.97 Å. It is evident in the optimized structure that the chloride ligand being at the *trans* position of the V=O is labile with a V–Cl bond length of 2.57 Å. This explains the dissociation of the chloride ligand in aqueous solution phase as is evidenced from the ESI-MS and molar conductivity data. The dihedral angle between the phenazine ring and the acridine moiety is 68.5° and this does not allow any effective $\pi$ conjugation between two planar chromophores. In both the structures, the HOMO is concentrated over the curcumin moiety, whereas the LUMO is located over the phenazine ring.

### *Cytotoxicity*

Photocytotoxicity of the complexes **1**–**3** was studied on human skin keratinocyte cell line (HaCaT) and human cervical cancer cell line (HeLa) using an MTT [3-(4,5-dimethylthiazole-2-yl)2,5-diphenyltetrazolium bromide] assay.[31] We have used the HaCaT cell line to know about the efficacy of the complexes in PDT and HeLa is used as a normal cancer cell line. The complexes were incubated for 4 h followed by photo-irradiation in visible light (400–700 nm photoreactor, 10 J·cm$^{-2}$) for 1.0 h (Figure 4). The $IC_{50}$ values of complex **1** were found to be 0.34(±0.03) μM in HaCaT and 0.99(±0.05) μM in HeLa cells. This complex showed no dark cytotoxicity in both the cell lines. The $IC_{50}$ values of complex **2** in light were 0.18(±0.02) μM in HaCaT and 0.71(±0.07) μM in HeLa cells. Complex **3** having a curcumin derivative containing a sugar moiety gave $IC_{50}$ values of 0.13(±0.03) μM in HaCaT and 0.33(±0.02) μM in HeLa cells. One reason for the higher photocytotoxicity of complex **3** may be the presence of the sugar moiety, which possibly increases the cellular uptake of this complex in the cancer cells. Com-

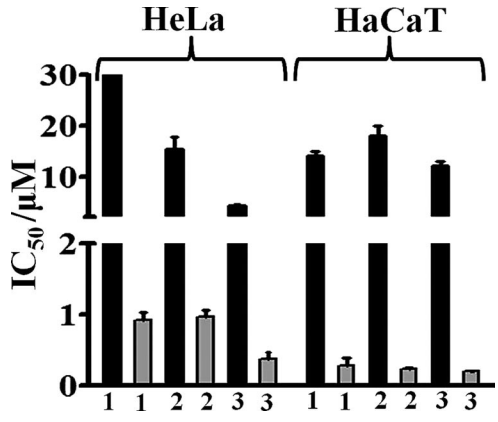


**Figure 4.** Photocytotoxicity of the complexes **1**–**3** from the MTT assay in HeLa and HaCaT cells on 4 h incubation in dark (black bar) and in visible light of 400–700 nm (gray bar).

Dedicated Issue

  

**Table 2.** The $IC_{50}$ /μM values of **1**–**3** and selected compounds in HaCaT and HeLa cells.

| Compound | HaCaT in visible light [a] | in dark | HeLa in visible light [a] | in dark |
|---|---|---|---|---|
| **1** | 0.34(±0.03) | >30 | 0.99(±0.05) | >30 |
| **2** | 0.18(±0.02) | >10 | 0.71(±0.07) | >10 |
| **3** | 0.13(±0.03) | 11.8(±0.6) | 0.33(±0.02) | 4.2(±0.1) |
| acdppz | >10 | >10 | 9.5(±0.3) | >20 |
| Hscur | >50 | >50 | >50 [b] | >50 |
| Curcumin | 19.0(±0.2) | 28.1(±0.4) | 8.2±(0.2) [c] | 85.4(±0.6) |
| Photofrin® [d] | | | 4.3 ± 0.2 [e] | >41 |

a) Light of 400–700 nm wavelength. b) Data from Ref. [7b]. c) Data from Ref. [8]. d) Data from Ref. [21]. e) Red light of 633 nm.

plex **3**, however, showed undesirable dark cytotoxicity giving $IC_{50}$ values of 11.8(±0.6) μM in HaCaT and 4.23(±0.08) μM in HeLa cells. This could be due to higher cellular uptake of the complex. Cytotoxicity of the ligands, viz. curcumin, sugar-appended curcumin, and acridine-dppz was measured and the data are given in Table 2. The complexes showing photocytotoxicity in nanomolar concentration with minimal dark toxicity are of importance in the chemistry of PDT.

### *Mechanistic Study of Cellular Damage*

DNA ladder assay is a convenient way to detect programmed cell death or apoptosis. Cellular apoptosis is due to the activation of endonuclease activity.[32] This activation leads to the degradation of genomic DNA at inter-nucleosomal linker region forming 180 to 185 base pair of DNA fragments. These DNA fragments can be analyzed by gel electrophoresis. We analyzed the mode of cell death from the DNA laddering experiment for complexes **1** and **2**. It is evident from Figure 5 that both the complexes show DNA ladder only in the presence of visible light (400–700 nm) in HaCaT cells indicating apoptosis as the primary mode of cell death. This experiment was also done for the complexes in HeLa cells, but only complex **2** gave ladder like pattern. No ladder formation was observed in dark indicating that the complexes become cytotoxic only on light exposure, while remaining innocuous to cells in dark. We probed generation of any reactive oxygen species (ROS) from 2′,7′-dichlorodihydrofluorescein diacetate (DCFDA) assay.[33] Cell permeable DCFDA could be oxidized by cellular ROS to generate fluorescent DCF with an emission maxima at 525 nm.[34] The percentage of cell population generating ROS could be determined by flow cytometry analysis. The assay data in HaCaT cell line indicate the formation of ROS by complex **2** on exposure to visible light, while there was no ROS formation in dark.

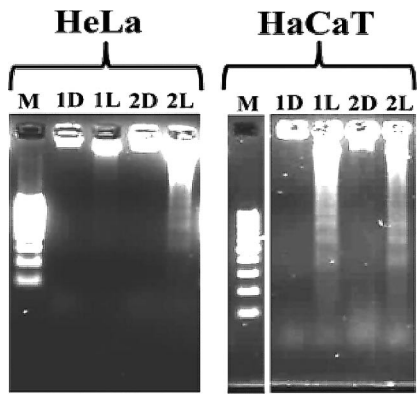


**Figure 5.** DNA ladder of the complexes **1** and **2** in HeLa and HaCaT cells showing apoptosis (D = dark, L = light, M = Marker 100 bp).

### *Cellular Imaging and Uptake*

The emission property of the complexes was used to study their cellular uptake and localization in the HaCaT and HeLa cells by confocal microscopy. Propidium iodide (PI) was used as a nuclear staining dye to ascertain any nuclear uptake of the complexes. Complexes **1**–**3** in HaCaT and HeLa cells showed significant accumulation within 2 h and were retained up to 4 h. The uptake of the complexes in 4 h was found to be more than that in 2 h. On comparing the merged image with the green fluorescence of the complex and red fluorescence of PI in Figure 6 (see Figure S18 for a colored image), complexes **1** and **2** were seen to localize mainly in the cytoplasm [panels (c), (f), (l) and (o)], whereas complex **3** localizes in the nucleus as well as in cytoplasm [panels (i) and (r)]. The nuclear morphology was found to remain intact as evident from the microscopy images indicating the nontoxic nature of the complexes in dark. The results are indeed remarkable since the complexes could serve the dual purpose of imaging the tumor for its detection and remaining passive within the cells in absence of light and become cytotoxic on photo-irradiation damaging the tumor.

Further study using mitochondrial tracker deep red in HaCaT cells showed partial localization of the complexes **1** and **2** in the mitochondria as evidenced from the yellow color in the merged image resulting from the green fluorescence of the complex and the red fluorescence of the mitotracker red (Figure 7, see Figure S19 for a colored image). We had to use low concentration of the complexes **1** and **2** to avoid any light-induced cell damage during the imaging experiments and this resulted in low fluorescence intensity. Complex **3** could not be used for imaging study due to its high cellular toxicity in dark.

### *DNA Binding Properties*

With the knowledge that the complexes partially localizing in the mitochondria and the mitochondrial DNA could be a possible site of binding, we investigated the DNA binding

  

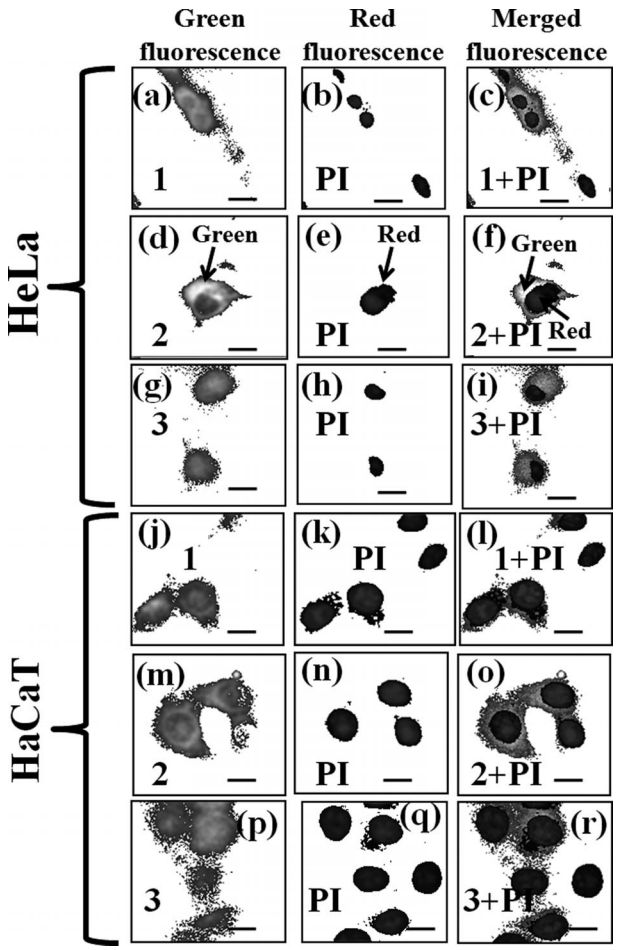


**Figure 6.** Confocal images of HeLa and HaCaT cells (after 4 h) treated with complexes **1–3** (10 μM) and propidium iodide (PI, 10 mg·mL$^{-1}$): panels (a), (d), (g), (j), (m) and (p) show the green emission of the complexes; panels (b), (e), (h), (k), (n), and (q) correspond to the red emission of PI; and panels (c), (f), (i), (l), (o) and (r) show the merged images. Scale Bar: 10 μm (for a colored image, see Figure S18).

strengths of the oxidovanadium(IV) complexes using absorption titration, DNA melting and viscosity measurements. The equilibrium binding constants ($K_b$) of the complexes **1–3** to ct-DNA were obtained from UV/Vis absorption titrations by monitoring the change in the absorbance of the ligand-based band of the complexes at 267 nm (ct-DNA = calf thymus DNA). Binding of a complex to DNA generally leads to hypochromism along with a bathochromic shift of the electronic spectral bands resulting from strong stacking interaction between the aromatic chromophore of the ligand in the complex and the base pairs of DNA.[35] The extent of hypochromism thus gives an estimate of the binding strength. The observed trend in hypochromism among the present oxidovanadium(IV) complexes follows the order: **3** > **2** > **1**. The equilibrium binding constant ($K_b$) values for the complexes range within $(3.1 \pm 0.2) \times 10^5$ to $(9.6 \pm 0.1) \times 10^5$ M$^{-1}$ giving the same order as observed in the trend of hypochromism (Table 1).

Thermal behavior of DNA in the presence of the complexes provides information on the conformational changes and the strength of the DNA complex interaction. The double-stranded

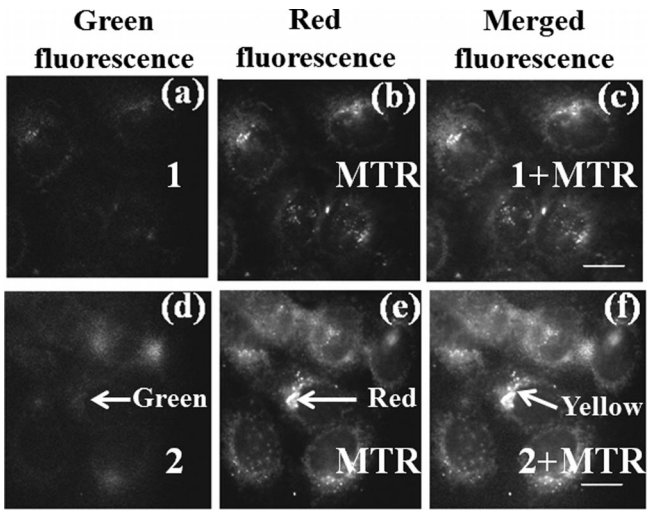


**Figure 7.** Confocal images of complexes **1** and **2** (10 μM) in HaCaT cells after 4 h showing the cellular uptake. Panels (a) and (d) show green fluorescence of complexes **1** and **2**, respectively. Panels (b) and (e) are red fluorescence images of mitotracker red (MTR, 50 nM). Panels (c) and (f) are the merged fluorescence images of the mitotracker and the complex. Scale Bar: 10 μm (for a colored image, see Figure S19).

DNA gradually dissociates to single strands on increasing the solution temperature. The melting temperature $T_m$ which is defined as the temperature where half of the total base pairs gets non-bonded is a valuable parameter. The DNA melting studies in phosphate buffer (pH 7.2) showed stabilizing interaction of all the complexes with ct-DNA (Table 1, Figure 8). The $\Delta T_m$ values for the complexes lie in the range of 5.1 to 7.4 °C and it is 10.6 °C for the DNA intercalator ethidium bromide (EB).[36] The ct-DNA binding strengths follow the order: **3** > **2** > **1**. The DNA melting data indicate intercalative mode of binding of the complexes to the ct-DNA.

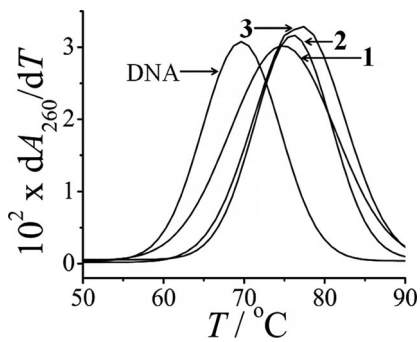


**Figure 8.** DNA melting plots of 190 μM ct-DNA alone and in the presence of **1–3** (20 μM) in 5 mM phosphate buffer (pH 7.2).

Viscosity measurements were carried out to examine the effect on the specific relative viscosity of ct-DNA upon addition of the complexes. DNA intercalating compounds result in a change in the relative viscosity by unwinding and elongation of the DNA double helix. For example, EB shows significant increase in the relative viscosity of the ct-DNA solution on intercalation due to an increase in the overall DNA contour

Dedicated Issue

  

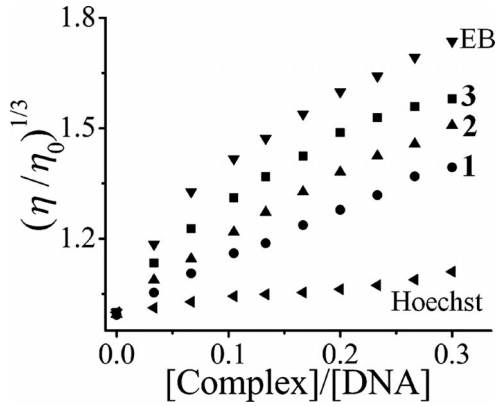


**Figure 9.** Plots showing the effect of increasing the concentration of ethidium bromide (EB) (▼), **1** (●), **2** (▲), **3** (■), and Hoechst 33258 (◀) on the relative viscosity of ct-DNA (150 μM) at 37.0 ± 0.1 °C in Tris-HCl buffer (5 mM, pH 7.2).

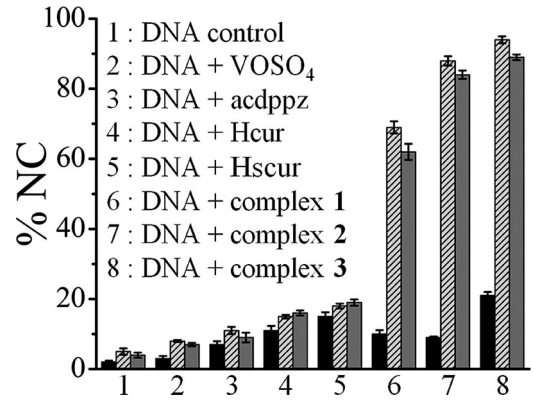


**Figure 10.** Bar diagram showing the photocleavage of SC pUC19 DNA (30 μM) by the ligands and the complexes **1–3** (30 μM). The reactions conditions are: in dark shown by black bars, in red light of 705 nm shown by shaded bars with stripes and in red light of 785 nm showing dark shaded bars.

length. In contrast, groove binding or partially intercalating molecules cause little or no effect on the relative viscosity of the ct-DNA solution.[37] The groove binder Hoechst 33258, used as a reference compound, showed no apparent change in the DNA solution viscosity. The plots of relative viscosity $(\eta/\eta_0)^{1/3}$ vs. [complex]/[DNA] ratio for **1–3**, where η and $\eta_0$ are respective specific viscosity of DNA in the presence and absence of the complexes show significant change in the relative specific viscosity (Figure 9). Comparison of the viscosity data with EB and Hoechst dye indicates partial intercalative binding nature of complex **1** to ct-DNA, whereas complexes **2** and **3** show significant intercalative ct-DNA binding.

### *Photoinduced DNA Cleavage*

The photocytotoxic effect of the complexes in the cancer cells and their mitochondrial and nuclear (for complex **3**) uptake prompted us to study their ability to photo-cleave supercoiled DNA in near-IR light. The photoactivated DNA cleavage activity of the complexes was studied using supercoiled (SC) pUC19 DNA in a medium of Tris-HCl/NaCl buffer on irradiation using near-IR light diode lasers of 705 nm and 785 nm wavelengths (Figure 10). The choice of these wavelengths is due to the presence of a central metal atom d-d absorption band near 725 nm in the electronic spectra of the complexes. The complexes displayed excellent DNA cleavage activity at these wavelengths even at very low complex concentration. A 30 μM solution of **2** induced ca. 85% DNA cleavage on exposure for 1 h. Complex **3** showed 92% cleavage of the SC DNA to its nicked circular (NC) form under similar reaction conditions (Table 3). Control experiments in dark did not show any significant DNA cleavage activity. The curcumin and glycosylated curcumin ligands alone showed 17% cleavage of SC DNA at these wavelengths. The photoactivity could be metal-assisted and involves the metal-based d–d band resulting in an excited state that generates the cleavage active species. The results showing DNA cleavage activity of the oxidovanadium(IV) complexes in near-IR light are of significant importance in PDT considering that the vanadium(V) complexes lacking any low energy electronic band are unsuitable for PDT application.[38]

The mechanistic aspects of the DNA photocleavage reactions in red light of 705 nm and 785 nm were studied using complexes **2** and **3** in the presence of various external additives. The complexes did not show any apparent DNA photocleavage activity in an argon atmosphere suggesting the necessity of $O_2$ to generate the ROS. The ROS could be hydroxyl radical species generated from a photo-redox process or singlet oxygen from the energy transfer type-II pathway. The addition of singlet oxygen quenchers, viz. sodium azide or TEMP showed significant reduction in the DNA cleavage activity in red light (Figure 11). Hydroxyl radical scavengers, viz. DMSO and KI had no apparent effect on the DNA cleavage activity of the complexes. Hydrogen peroxide and superoxide anion

**Table 3.** Selected SC pUC19 DNA (0.2 μg) cleavage data of **1–3** and the ligands in red light.

| Reaction conditions [a] | % NC Form (in dark) | % NC Form (red light, 705 nm) | % NC Form (red light, 785 nm) |
|---|---|---|---|
| DNA control | 2 | 5 | 4 |
| DNA + **1** | 10 | 69 | 62 |
| DNA + **2** | 9 | 88 | 84 |
| DNA + **3** | 21 | 94 | 89 |
| DNA + curcumin (Hcur) | 11 | 15 | 16 |
| DNA + Hscur | 15 | 18 | 19 |

a) In Tris-buffer medium (pH = 7.2). Red light from diode lasers. Photo-exposure time (*t*) = 1 h. Concentration of the complexes **1–3** and the ligands used was 30 μM.

  

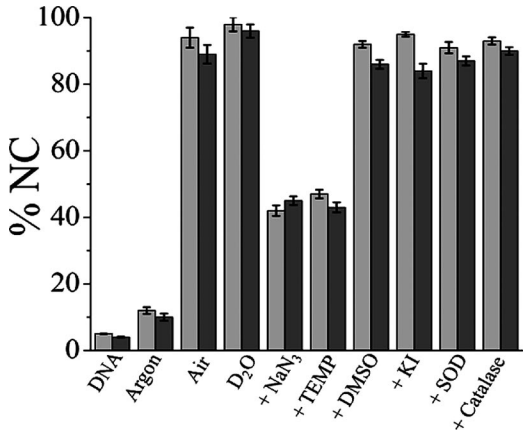


**Figure 11.** Bar diagram showing the extent of photocleavage of pUC19 DNA (0.2 μg, 30 μM) by complex **3** (30 μM) forming nicked circular (NC) form of DNA in the presence of additives in red light of 705 nm (light shade) and 785 nm (dark shade) for an exposure time of 1 h [$D_2O$, 16 μL; $NaN_3$, 0.5 mM; TEMP, 0.5 mM; DMSO, 4 μL; KI, 0.5 mM; SOD, 4 units; catalase, 4 units].

radical scavengers, viz. catalase and SOD did not show any inhibitory effect. The results suggest the involvement of singlet oxygen ($^1O_2$) in the photocleavage reaction, which was further confirmed from our observation of enhanced DNA photocleavage activity in $D_2O$ due to longer lifetime of $^1O_2$ in this solvent.[39,40] The DNA cleavage reaction involving molecular oxygen ($^3O_2$) seems to proceed via a type-II process, in which the excited electronic state of the complex through efficient intersystem crossing generates the triplet excited state of the photo-sensitizer that activates triplet oxygen to the reactive singlet state by energy transfer.

## Conclusions

We report remarkable visible light-induced photocytotoxicity of a new class of curcumin-based oxidovanadium(IV) complexes in a ternary structure having 11-(9-acridinyl)dipyrido[3,2-a:2′,3′-c]phenazine base, while being less toxic in dark. The photocytotoxicity of the complexes is higher than that of the PDT drug Photofrin®. The complexes showed DNA photocleavage activity in near-IR light via singlet oxygen pathway and cellular damage via apoptotic pathway. The DNA melting and viscosity data show intercalative mode of DNA binding of the complexes. The complexes do not show any apparent chemical nuclease activity due to their redox stability over a wide potential range. Confocal studies reveal mainly cytosolic localization of the complexes **1** and **2** in cancer cells with significant mitochondrial uptake. The results showing dual effect of the complexes in cellular imaging and light-induced apoptosis by targeting mitochondria caused by singlet oxygen generation are distinctly different from the known metal-based PDT agents.

Complex **2** is unique in the chemistry of metal-based PDT agents having excellent functional similarities with the PDT drug Photofrin®, viz. (i) visible light-induced photo-cytotoxicity with low dark toxicity, (ii) singlet oxygen ($^1O_2$) as the ROS, (iii) apoptotic cell death, (iv) DNA binding and photo-induced DNA cleavage activity in red light, (v) cytosolic localization, and (vi) significant mitochondrial uptake. This work is expected to presage designing and developing new generation of mitochondria targeting metal-based PDT and tumor imaging agents for their potential applications in PDT.

## Experimental Section

**Materials:** All reagents and chemicals were procured from commercial sources (s.d. Fine Chemicals, India; Aldrich, USA) and used without further purification. Curcumin (95% curcuminoid content, 80% curcumin) was purchased from Sigma-Aldrich and purified into individual components by following a reported procedure.[41] Solvents were purified by standard procedures.[42] Supercoiled (SC) pUC19 DNA (cesium chloride purified) was purchased from Bangalore Genie (India). Tris-(hydroxymethyl)aminomethane-HCl (Tris-HCl) buffer solution was prepared using deionized and sonicated triple distilled water. Calf thymus (ct) DNA, agarose (molecular biology grade), distamycin, catalase, superoxide dismutase (SOD), ethidium bromide (EB), 3-(4,5-dimethylthiazol-2-yl)-2,5-diphenyltetrazolium bromide (MTT) and 2′,7′-dichlorofluorescein diacetate (DCFDA) were procured from Sigma (USA). MitoTracker® Deep Red FM (Cat. no.M22426) (MTR) was purchased from Invitrogen BioServices India. 11-(9-Acridinyl)dipyrido[3,2-a:2′,3′-c]phenazine (acdppz) ligand was prepared following a literature procedure using 1,10-phenanthroline-5,6-dione as a precursor.[20] The glycosylated curcumin, viz., diglucosylcurcumin (Hscur) and 1,7-bis(3-methoxy-4-β-D-glucopyranos-1-yloxophenyl)hepta-1,6-diene-3,5-dione, was prepared according to a literature method.[18] Synthesis of the complexes was carried out in a nitrogen atmosphere using Schlenk technique. Tetrabutylammonium perchlorate (TBAP) was prepared using tetrabutylammonium bromide and perchloric acid.

**Instrumentation:** The elemental analysis was done with a Thermo Finnigan FLASH EA 1112 CHNS analyzer. The infrared and electronic spectra were recorded with a Perkin-Elmer Lambda 35 and a Perkin-Elmer spectrum one 55, respectively, at 25 °C. Molar conductivity measurements were done with a Control Dynamics (India) conductivity meter. Electrochemical measurements were made at 25 °C with an EG&G PAR model 253 VersaStat potentiostat/galvanostat with electrochemical analysis software 270 using a three electrode setup consisting of a glassy carbon working, platinum wire auxiliary and a saturated calomel reference electrode (SCE) in 20% DMF-$H_2O$. TBAP (0.1 M) was used as a supporting electrolyte for the electrochemical measurements. Electrospray ionization (ESI) mass spectral measurements were made with a Bruker Daltonics make Esquire 300 Plus ESI model. The NMR spectra were recorded with a Bruker Avance 400 (400 MHz) NMR spectrometer. Room temperature fluorescence quantum yield measurements were done with a Perkin-Elmer LS 55 fluorescence spectrometer using coumarin-153 laser dye as a reference with a known Φ value of 0.56 in acetonitrile.[43] Samples were deaerated prior to spectral measurements. The complexes and reference were excited at 390 nm, maintaining nearly equal absorbance and the emission spectra were recorded from 410 to 650 nm. The integrated emission intensity was calculated using Origin Pro 8.1 software and the quantum yield was calculated using the equation: $(\Phi_S/\Phi_R) = (A_S/A_R)\times((OD)_S/(OD)_R)\times(n_S^2/n_R^2)$, where $\Phi_S$ and $\Phi_R$ are the fluorescence quantum yields of the sample and reference respectively, $A_S$ and $A_R$ are the area under the fluorescence spectra of the sample and the reference respectively, $(OD)_S$ and $(OD)_R$ are the respective optical densities of the sample and the reference solution at the wavelength of excitation, and $n_S$ and $n_R$ are the refractive indices for the respective solvents

Dedicated Issue

  

used for the sample and the reference.[44,45] Room temperature magnetic moment of the [$D_6$]DMSO solutions of the oxidovanadium(IV) complexes containing 1% TMS (v/v) as the internal reference was obtained by a solution NMR method with a Bruker AMX-400 NMR spectrometer.[46,47] Fluorescence microscopic investigations were carried out with a Leica DM IL microscope with integrated Leica DFC400 camera and IL50 image software. Confocal microscopy was done using confocal scanning electron microscope (Leica, TCS SP5 DM6000).

**Synthesis of [VO(acac)(L)Cl] (1), [VO(cur)(L)Cl] (2), and [VO(scur)(L)Cl] (3) (L = acdppz):** Vanadyl sulfate (0.16 g, 1.0 mmol) and barium chloride (0.25 g, 1.0 mmol) together were dissolved in aqueous ethanol (24 mL, 1:5 v/v). The mixture was stirred at 25 °C for 2 h in a nitrogen atmosphere using Schlenk technique. The mixture was filtered using celite to remove the barium sulfate precipitate. The blue filtrate was de-aerated and saturated with nitrogen. The acdppz base (0.46 g, 1.0 mmol) taken in chloroform-ethanol (20 mL, 2:3 v/v) was added to the filtrate. A deep greenish solution was formed after stirring the mixture for 10 min. Ligand Hacac or curcumin (Hcur) or glycosylated curcumin (Hscur) [Hacac, 0.10 g, Hcur, 0.36 g, Hscur, 0.69 g (1.0 mmol)] taken in acetonitrile-ethanol mixture (16 mL, 1:3 v/v), neutralized with $Et_3N$ (0.10 g, 1.0 mmol), was added to the previously formed deep greenish solution. The complex as a precipitate was obtained after stirring the solution for 2 h in nitrogen atmosphere. The precipitate was filtered, isolated, washed with cold acetonitrile, ethanol, THF, chloroform, and diethyl ether and finally dried in vacuo over $P_4O_{10}$ (Yield: ca. 78% for **1**; 81% for **2**, and 72% for **3**).

**Complex 1:** (M = 660.10), $C_{36}H_{24}N_5ClO_3V$: calcd. C 65.41; H 3.66; N 10.60%; found: C 65.32; H 3.61; N 10.68%. **ESI-MS** ($CH_3OH$): *m/z* 625.56 $[M - Cl]^+$. **IR**: $\tilde{\nu}$ = 3062 w, 1591 s, 1495 vs, 1420 s, 1383 m, 1277 s, 1150 m, 1121 m, 1035 w, 965 m, 841 m, 719 m, 557 w, 459 w $cm^{-1}$ (vs, very strong; s, strong; m, medium; w, weak). **UV/Vis** (20% DMF-water) [$\lambda_{max}$ /nm ($\varepsilon$ /$dm^3 \cdot M^{-1} \cdot cm^{-1}$)]: 717 (47), 387 (19 860), 362 (19 500), 269 (62 750). $\Lambda_M$ = 111 $S \cdot m^2 \cdot M^{-1}$ in 20% aqueous DMF at 25 °C. $\mu_{eff}$, $\mu_B$ at 298 K: 1.63.

**Complex 2:** (M = 928.17), $C_{52}H_{36}N_5ClO_7V$: calcd. C 67.21; H 3.90; N 7.54%; found: C 67.30; H 3.86; N 7.59%. **ESI-MS** ($CH_3OH$): *m/z* 893.20 $[M - Cl]^+$. **IR**: $\tilde{\nu}$ = 3069 w, 1586 s, 1492 vs, 1422 s, 1379 m, 1277 s, 1153 m, 1119 m, 1030 w, 967 m, 810 m, 721 m, 560 w, 462 w, 436 m $cm^{-1}$. **UV/Vis** (20% aqueous DMF) [$\lambda_{max}$ /nm ($\varepsilon$ /$dm^3 \cdot M^{-1} \cdot cm^{-1}$)]: 725 (51), 454 sh (56 830), 437 (57 370), 389 (46 170), 362 (34 600), 267 (77 800). $\Lambda_M$ = 92 $S \cdot m^2\ M^{-1}$ in 20% aqueous DMF at 25 °C. $\mu_{eff}$, $\mu_B$ at 298 K: 1.65.

**Complex 3:** (M = 1252.28), $C_{64}H_{56}N_5ClO_{17}V$: calcd. C 61.32; H 4.50; N 5.59%; found: C 61.44; H 4.57; N 5.52%. **ESI-MS** ($CH_3OH$): *m/z* 1217.23 $[M - Cl]^+$. **IR**: $\tilde{\nu}$ = 3301 br, 1589 s, 1504 vs, 1423 w, 1384 w, 1276 s, 1126 m, 1071 m, 1030 m, 962 m, 817 w, 725 w, 551 w, 466 w (br., broad) $cm^{-1}$. **UV/Vis** (20% DMF-water) [$\lambda_{max}$ /nm ($\varepsilon$ /$dm^3 \cdot M^{-1} \cdot cm^{-1}$)]: 729 (54), 427 (52 760), 391 (47 510), 363 (36 490), 266 (71 350). $\Lambda_M$ = 81 $S \cdot m^2 \cdot M^{-1}$ in 20% aqueous DMF at 25 °C. $\mu_{eff}$, $\mu_B$ at 298 K: 1.62.

**Solubility and Stability:** The complexes showed good solubility in DMF, DMSO, MeOH, moderate solubility in water, ethanol, acetonitrile, and poor solubility in hydrocarbons. The diglucosylcurcumin complex **3** having the carbohydrate moiety showed better solubility in water than the curcumin complex **2**. The complexes were found to be stable in solution in the monocationic form. The solution stability of the cationic species was ascertained from their time dependent molar conductivity and electronic absorption spectroscopic data. The absorption spectral study using curcumin and its derivative alone showed gradual degradation with time resulting to almost complete degradation in 24 h as evidenced from the decrease in the intensity of the absorption spectral band at 435 nm with the appearance of a new band at 252 nm in DMSO-phosphate buffer (1:1 v/v, pH = 7.2 at 37 °C). The oxidovanadium(IV) complexes of these ligands did not show any apparent spectral change even after 48 h.

**Cell Culture:** HeLa (human cervical carcinoma) cancer cells and HaCaT (human skin keratinocyte) cells were maintained in Dulbecco's Modified Eagle's Medium (DMEM), supplemented with 10% fetal bovine serum (FBS), 100 IU $mL^{-1}$ of penicillin, 100 $\mu g \cdot mL^{-1}$ of streptomycin and 2 mM Glutamax at 37 °C in a humidified incubator at 5% $CO_2$. The adherent cultures were grown as monolayer and passaged once in 4–5 d by trypsinizing with 0.25% Trypsin-EDTA.

**Cell Viability Assay:** The photocytotoxicity of the complexes **1–3** was studied using MTT assay, which is based on the ability of mitochondrial dehydrogenases of viable cells to cleave the tetrazolium rings of MTT resulting formation of dark purple membrane impermeable crystals of formazan that could be quantified from spectral measurements in DMSO.[31] Approximately, 8000 cells of HeLa and HaCaT were plated in a 96 wells culture plate in Dulbecco's Modified Eagle Medium (DMEM) containing 10% fetal bovine serum (FBS) and kept for 24 h incubation at 37 °C in a $CO_2$ incubator. The stock solution of the complexes, prepared in DMSO, was first diluted in the culture medium to the desired concentration and next added to the 96 well plates keeping the quantity of DMSO constants at 1% for all tests. Cells were incubated for 4 h in dark. The medium that was subsequently replaced with PBS was photo-irradiated with visible light (400–700 nm) for 1 h using a Luzchem Photoreactor (Model LZC-1, Ontario, Canada) fitted with Sylvania make 8 fluorescent white tubes with a fluence rate of 2.4 $mW \cdot cm^{-2}$ to provide a total dose of 10 $J \cdot cm^{-2}$. After photoexposure, PBS was removed and replaced with DMEM-FBS and incubation was continued for further 20 h in dark. After the incubation period, 20 µL of 5 $mg \cdot mL^{-1}$ of MTT was added to each well and incubated for an additional 3 h. The culture medium was finally discarded and 200 µL of DMSO was added to dissolve the formazan crystals and its absorbance at 595 nm was measured using a BIORAD ELISA plate reader. Cytotoxicity of **1–3** was measured as the percentage ratio of the absorbance of the treated cells to the untreated controls. The $IC_{50}$ values were determined by nonlinear regression analysis (GraphPad Prism).

**DNA Fragmentation Analysis by Agarose Gel Electrophoresis:** The DNA fragmentation assay was performed to observe any apoptotic mode of cell death induced by complexes **1** and **2** using HeLa and HaCaT cells.[48] Briefly, $0.3 \times 10^6$ cells were taken in each 60 mm dish, grown for 24 h and later treated with **1** (2 µM) and **2** (1 µM) incubated for 4 h in dark. One dish containing the complex was exposed to light for 1 h and again the cells were left to grow for 4 h along with its dark control in another dish. After 4 h, cells were trypsinized, washed with DPBS and re-suspended in 0.4 mL of lysis buffer (10 mM Tris-HCl; pH, 8.0, 20 mM EDTA, 0.2% triton-X 100) with incubation for 20 min on ice. Lysed cells were centrifuged for 20 min at 13000 rpm and the supernatant having soluble chromosomal DNAs including both high molecular weight DNA and nucleosomal DNA fragments was collected. Phenol chloroform was performed to remove the protein present. Later supernatant was precipitated with 1/10 volume of 3 M sodium acetate (pH 5.8) and 2 volume of ethanol at –20 °C for overnight. DNA pellet was washed with 70% alcohol and re-suspended in Tris-EDTA (pH 8) containing RNAse (100 $\mu g \cdot mL^{-1}$) followed by incubation at 37 °C for 2 h. DNA samples were resolved on



  

1.5% agarose gel at 80 V for about 2 h and photographed under UV light.

**DCFDA Assay for Measurement of ROS Generation:** DCFDA assay was used to detect the formation of any reactive oxygen species (ROS) in the cancer cells. Cell permeable DCFDA on oxidation by cellular ROS generates DCF as green fluorescent compound. The percentage of cells generating ROS was determined by flow cytometry analysis. To detect ROS generation, HaCaT cells were incubated with complex **2** (1 μM) for 4 h followed by photo-irradiation (400–700 nm) for 1 h in serum free conditions. The cells were harvested by trypsinization and a single cell suspension of $1 \times 10^6$ cells·mL$^{-1}$ was prepared. The cells were treated with 1 μM DCFDA solution in DMSO in dark for 20 min at room temperature. The distribution of DCFDA stained HaCaT cells was determined by flow cytometry in the FL-1 channel.

**Confocal Studies: Uptake and Localization:** Uptake and localization of fluorescent complexes into the cell was visualized using a confocal scanning electron microscope (Zeiss, LSM510 apocromat).[49] HeLa and HaCaT cells were grown on glass cover slips in each 12 well plates at a seeding density of 50,000 cells in 1.5 mL of culture medium for 24 h. Cells were treated with the complexes for 2 h and 4 h in dark, fixed, and permeabilized with chilled methanol for 5 min at –20 °C. Methanol was subsequently removed followed by washing with 1X PBS buffer. It was later incubated with propidium iodide (1 mg·mL$^{-1}$) to stain the nucleus for 2 min and visualized under a confocal scanning electron microscope. The cell-permeant MitoTracker® deep red having a mildly thiol-reactive chloromethyl moiety was used for labeling mitochondria. A 50 nM of MitoTracker® Deep Red FM (Cat. no.M22426) was used for confocal microscopy.[22a]

**DNA Binding Methods:** The experiments were done in Tris-HCl buffer (5 mM, pH 7.2) using DMF solution of the complexes **1**–**3**. Calf thymus (ct) DNA (ca. 350 μM NP, nucleotide pair) in this buffer medium gave a ratio of UV absorbance at 260 and 280 nm of ca. 1.9:1 indicating the DNA apparently free from any protein impurity. The concentration of ct-DNA was estimated from its absorption intensity at 260 nm with a molar extinction coefficient value ($\varepsilon$) of 6600 dm$^3$·M$^{-1}$·cm$^{-1}$.[50,51] Absorption titration experiments were done by changing the concentration of ct-DNA while maintaining constant complex concentration following a method as reported earlier.[16,17] The intrinsic equilibrium binding constant ($K_b$) of the complexes **1**–**3** to ct-DNA were obtained by the McGhee-von Hippel (MvH) method.[52,53] DNA thermal denaturation studies were carried out by monitoring the absorption intensity of ct-DNA (190 μM) at 260 nm by varying the temperature from 40 to 90 °C in both absence and presence of the complexes (**1**–**3**) (20 μM) using a Cary 300 bio UV/Vis spectrometer with a Cary temperature controller at an increase rate of 0.5 °C per min of the solution. The viscosity measurements were done using a Schott Gerate AVS. 310 automated viscometer attached to a constant temperature bath at 37 °C. The concentration of the ct-DNA stock solution was 150 μM (NP) in a 5 mM Tris-HCl buffer. The complex was added gradually on increasing the concentration from 0 to 120 μM, and the viscosity was measured on each addition. The flow times were monitored with an automated timer. The relative specific viscosity of DNA, $(\eta/\eta_0)^{1/3}$ was plotted vs. [complex]/[DNA], where $\eta$ is the viscosity of DNA in the presence of the complex and $\eta_0$ is the viscosity of ct-DNA alone in 5 mM Tris buffer medium. The viscosity values were calculated from the observed flow time of ct-DNA containing solutions ($t$), duly corrected for that of the buffer alone ($t_0$), $\eta = (t - t_0)/t_0$.

**DNA Cleavage Methods:** The cleavage of supercoiled (SC) pUC19 DNA (0.2 μg, 30 μM, 2686 base-pairs) was studied by agarose gel electrophoresis using the complexes in 50 mM Tris-HCl buffer (pH 7.2) and 50 mM NaCl containing 10% DMF. The photo-induced DNA cleavage reactions were carried out in red light using diode lasers of 705 nm and 785 nm wavelengths (Model: LQC705-38E and LQC785-100C from Newport Corporation). The laser powers were 38 mW and 100 mW, respectively, measured using Spectra Physics CW laser power meter (Model 407A). Prior to light exposure, each sample was incubated for 1.0 h at 37 °C and the photo-cleaved products were analyzed by gel electrophoresis as reported earlier.[54] The mechanistic studies were carried out using different additives ($NaN_3$, 0.5 mM; DMSO, 4 μL; KI, 0.5 mM; catalase, 4 units; SOD, 4 units; TEMP, 0.5 mM). For the $D_2O$ experiment, this solvent was used to dilute the sample up to 20 μL final volume. The extent of SC DNA cleavage was measured from the intensities of the bands using UVITEC Gel Documentation System. Due corrections were made for the low level of nicked circular (NC) form of DNA present in the original SC DNA sample and for the low affinity of EB binding to SC compared to NC form of DNA.[55] The observed error in measuring the band intensities was ca. 5%.

**Supporting Information** (see footnote on the first page of this article): The supplementary data contain ESI-MS (Figures S1–S3), IR (Figures S4–S6), cyclic voltammograms (Figure S7), energy optimized geometry and HOMO-LUMO diagrams (Figures S8–S10), MTT plot (Figures S11–S16), DCFDA assay (Figure S17), confocal images (Figure S18–S20), DNA binding plots (Figure S21), DNA cleavage data (Figures S22–S25), spectroscopic data for measuring stability (Figure S26) and computational data for the complexes (Tables S1 and S2).

## Acknowledgements

*A.R.C.* thanks the Department of Science and Technology (DST, Government of India), and the Council of Scientific and Industrial Research, New Delhi), for financial support (SR/S5/MBD-02/2007 and CSIR/01(2559)/12/EMR-II/2012) and DST for J.C. Bose fellowship. We are thankful to the Alexander von Humboldt Foundation for donation of an electrochemical system and Mr. Sanjoy Mukherjee for his help in computational studies. *S.B.* thanks the University Grants Commission (UGC), New Delhi, for a fellowship.

## References

[1] a) H. Hatcher, R. Planalp, J. Cho, F. M. Torti, S. V. Torti, *Cell Mol. Life Sci.* **2008**, *65*, 1631–1652; b) V. S. Govindarajan, W. H. Stahl, *Crit. Rev. Food Sci. Nutr.* **1980**, *12*, 199–301.

[2] B. B. Aggarwal, C. Sundaram, N. Malani, H. Ichikawa, *Adv. Exp. Med. Biol.* **2007**, *595*, 1–75.

[3] a) C. H. Hsu, A. L. Cheng, *Adv. Exp. Med. Biol.* **2007**, *595*, 471–480; b) B. B. Aggarwal, A. Kumar, A. C. Bharti, *Anticancer Res.* **2003**, *23*, 363–398; c) M.-H. Teiten, S. Eifes, M. Dicato, M. Diederich, *Toxins* **2010**, *2*, 128–162.

[4] P. Anand, S. G. Thomas, A. B. Kunnumakkara, C. Sundaram, K. B. Harikumar, B. Sung, S. T. Tharakan, K. Misra, I. K. Priyadarsini, K. N. Rajasekharan, B. B. Aggarwal, *Biochem. Pharmacol.* **2008**, *76*, 1590–1611.

[5] T. Choudhuri, S. Pal, M. L. Agwarwal, T. Das, G. Sa, *FEBS Lett.* **2002**, *512*, 334–340.

[6] R. A. Sharma, W. P. Steward, A. J. Gescher, *Adv. Exp. Med. Biol.* **2007**, *595*, 453–470.

[7] a) D. Pucci, T. Bellini, A. Crispini, I. D′Agnano, P. F. Liguori, P. Garcia-Orduña, S. Pirillo, A. Valentini, G. Zanchetta, *Med. Chem. Commun.* **2012**, *3*, 462–468; b) A. Hussain, K. Somyajit, B. Banik, S. Banerjee, G. Nagaraju, A. R. Chakravarty, *Dalton Trans.* **2013**, *42*, 182–195; c) A. K. Renfrew, N. S. Bryce, T. W. Hambley, *Chem. Sci.* **2013**, *4*, 3731–3739.

Dedicated Issue

  

[8] S. Banerjee, P. Prasad, A. Hussain, I. Khan, P. Kondaiah, A. R. Chakravarty, *Chem. Commun.* **2012**, *48*, 7702–7704.
[9] a) I. K. Priyadarsini, *J. Photochem. Photobiol. C: Photochem. Rev.* **2009**, *10*, 81–95; b) T. A. Dahl, P. Bilski, K. J. Reszka, C. F. Chignell, *Photochem. Photobiol.* **1994**, *59*, 290–294.
[10] M. J. Clarke, F. Zhu, D. R. Frasca, *Chem. Rev.* **1999**, *99*, 2511–2533.
[11] a) D. C. Crans, A. S. Tracey in *Vanadium Compounds: Chemistry, Biochemistry, and Therapeutic Applications* (Eds.: A. S. Tracey, D. C. Crans), American Chemical Society, Washington, DC, **1998**, vol. 711, pp 2–29; b) D. Rehder, J. C. Pessoa, C. F. G. C. Geraldes, M. M. C. A. Castro, T. Kabanos, T. Kiss, B. Meier, G. Micera, L. Pettersson, M. Rangel, A. Salifoglou, I. Turel, D. Wang, *J. Biol. Inorg. Chem.* **2002**, *7*, 384–396.
[12] J. Kuwahara, T. Suzuki, Y. Sugiura, *Biochem. Biophys. Res. Commun.* **1985**, *129*, 368–374.
[13] H. Sakurai, H. Tamura, K. Okatani, *Biochem. Biophys. Res. Commun.* **1995**, *206*, 133–137.
[14] C.-T. Chen, J.-S. Lin, J.-H. Kuo, S.-S. Weng, T.-S. Cuo, Y.-W. Lin, C.-C. Cheng, Y.-C. Huang, J.-K. Yu, P.-T. Chou, *Org. Lett.* **2004**, *6*, 4471–4474.
[15] a) D. W. J. Kwong, O. Y. Chan, R. N. S. Wong, S. M. Musser, L. Vaca, S. I. Chan, *Inorg. Chem.* **1997**, *36*, 1276–1277; b) C. Hiort, J. Goodisman, J. C. Dabrowiak, *Biochemistry* **1996**, *35*, 12354–12362.
[16] P. K. Sasmal, S. Saha, R. Majumdar, S. De, R. R. Dighe, A. R. Chakravarty, *Dalton Trans.* **2010**, *39*, 2147–2158.
[17] S. Banerjee, A. Hussain, P. Prasad, I. Khan, B. Banik, P. Kondaiah, A. R. Chakravarty, *Eur. J. Inorg. Chem.* **2012**, 3899–3908.
[18] a) E. Ferrari, S. Lazzari, G. Marverti, F. Pignedoli, F. Spagnolo, M. Saladini, *Bioorg. Med. Chem.* **2009**, *17*, 3043–3052; b) K. Mohri, Y. Watanabe, Y. Yoshida, M. Satoh, K. Isobe, N. Sugimoto, Y. Tsuda, *Chem. Pharm. Bull.* **2003**, *51*, 1268–1272.
[19] a) R. S. Brown, R. L. Wahl, *Cancer* **1993**, *72*, 2979–2985; b) S. N. Reske, K. G. Grillenberger, G. Glatting, M. Port, M. Hildebrandt, F. Gansauge, H. G. Beger, *J. Nucl. Med.* **1997**, *38*, 1344–1348.
[20] M. Mariappan, M. Suenaga, A. Mukhopadhyay, P. Raghavaiah, B. G. Maiya, *Inorg. Chim. Acta* **2011**, *376*, 340–349.
[21] E. Delaey, F. V. Laar, D. De Vos, A. Kamuhabwa, P. Jacobs, P. De Witte, *J. Photochem. Photobiol.* **2000**, *B55*, 27–36.
[22] a) M. Lam, N. L. Oleinick, A.-L. Nieminen, *J. Biol. Chem.* **2001**, *276*, 47379–47386; b) R. Hilf, *J. Bioenerg. Biomembr.* **2007**, *39*, 85–89; c) J. S. Armstrong, *Br. J. Pharmacol.* **2006**, *147*, 239–248; d) S. Fulda, L. Galluzzi, G. Kroemer, *Nat. Rev. Drug Discovery* **2010**, *9*, 447–467; e) C. E. Wenner, *J. Cell. Physiol.* **2012**, *227*, 450–456.
[23] J. Saczko, M. Mazurkiewicz, A. Chwilkowska, J. Kulbacka, G. Kramer, M. Ługowski, M. Śnietura, T. Banas, *Folia Biol.* **2007**, *53*, 7–12.
[24] a) S. Marrachea, S. Dhar, *Proc. Natl. Acad. Sci. USA* **2012**, *109*, 16288–16293; b) S. Marrachea, S. Tundup, D. A. Harn, S. Dhar, *ACS Nano* **2013**, *7*, 7392–7402.
[25] P. Prasad, I. Khan, P. Kondaiah, A. R. Chakravarty, *Chem. Eur. J.* **2013**, *19*, 17445–17555.
[26] N. A. Smith, P. J. Sadler, *Phil. Trans. R. Soc. A* **2013**, *371*, 20120519.
[27] a) W. J. Geary, *Coord. Chem. Rev.* **1971**, *7*, 81–122; b) I. Ali, W. A. Wani, K. Saleem, *Synthesis and Reactivity in Inorganic, Metal-Organic, and Nano-Metal Chemistry*, **2013**, 43, 1162–1170.
[28] K. Nakamoto, *Infrared and Raman Spectra of Inorganic and Coordination Compounds*, John Wiley & Sons, New York. **1997**.
[29] K. Toshima, R. Takano, T. Ozawa, S. Matsumura, *Chem. Commun.* **2002**, 212–213.
[30] a) A. D. Becke, *Phys. Rev.* **1998**, *A38*, 3098–3100; b) A. D. Becke, *J. Chem. Phys.* **1993**, *98*, 5648–5652; c) C. Lee, W. Yang, R. G. Parr, *Phys. Rev. B* **1988**, *37*, 785–789; d) P. J. Hay, W. R. Wadt, *J. Chem. Phys.* **1985**, *82*, 284–298.
[31] T. Mosmann, *J. Immunol. Methods* **1983**, *65*, 55–63.
[32] D. M. Conrad, S. J. Furlong, C. D. Doucette, K. A. West, D. W. Hoskin, *Apoptosis* **2010**, *15*, 597–607.
[33] A. S. Keston, R. Brandt, *Anal. Biochem.* **1965**, *11*, 1–5.
[34] T. Takanashi, Y. Ogura, H. Taguchi, M. Hashizoe, Y. Honda, *Investigative Ophthalmol. Vis. Sci.* **1997**, *38*, 2721–2728.
[35] R. B. Nair, E. S. Tang, S. L. Kirkland, C. J. Murphy, *Inorg. Chem.* **1998**, *37*, 139–141.
[36] M. Cory, D. Mckee, J. Kagan, D. Henry, J. Miller, *J. Am. Chem. Soc.* **1985**, *107*, 2528–2536.
[37] a) C. V. Kumar, E. H. Asuncion, *J. Am. Chem. Soc.* **1993**, *115*, 8541–8553; b) L. E. Gunther, A. S. Yong, *J. Am. Chem. Soc.* **1968**, *90*, 7323–7328; c) J. M. Veal, R. L. Rill, *Biochemistry* **1991**, *30*, 1132–1140; d) G. Cohen, H. Eisenberg, *Biopolymers* **1969**, *8*, 45–55.
[38] Y. Sun, Y. Zheng, W.-H. Lei, Q.-X. Zhou, Y.-J. Hou, B.-W. Zhang, X.-S. Wang, *Dalton Trans.* **2012**, *41*, 651–657.
[39] A. U. Khan, *J. Phys. Chem.* **1976**, *80*, 2219–2227.
[40] P. B. Merkel, D. R. Kearns, *J. Am. Chem. Soc.* **1972**, *94*, 1029–1030.
[41] O. Vajragupta, P. Boonchoong, L. Berliner, *Free Radic. Res.* **2004**, *38*, 303–314.
[42] D. D. Perrin, W. L. F. Armarego, D. R. Perrin in *Purification of Laboratory Chemicals*, Pergamon Press, Oxford, **1980**.
[43] J. Guilford II, R. Jackson, C. Choi, W. R. Bergmark, *J. Phys. Chem.* **1985**, *89*, 294–300.
[44] J. R. Lakowicz, *Principles of Fluorescence Spectroscopy*, Kluwer Academic/Plenum Publishers, New York, **1999**.
[45] A. T. R. Williams, S. A. Winfield, J. N. Miller, *Analyst* **1983**, *108*, 1067–1071.
[46] D. F. Evans, *J. Chem. Soc.* **1959**, 2003–2005.
[47] D. F. Evans, T. A. James, *J. Chem. Soc. Dalton Trans.* **1979**, 723–726.
[48] P. T. Daniel, I. Sturm, S. Ritschel, K. Friedrich, B. Dörken, P. Bendzko, T. Hillebrand, *Anal. Biochem.* **1999**, *266*, 110–115.
[49] T. Esteves, F. Marques, A. Paulo, J. Rino, P. Nanda, C. J. Smith, I. Santos, *J. Biol. Inorg. Chem.* **2011**, *16*, 1141–1153.
[50] S. P. Foxon, C. Metcalfe, H. Adams, M. Webb, J. A. Thomas, *Inorg. Chem.* **2007**, *46*, 409–416.
[51] M. E. Reichmann, S. A. Rice, C. A. Thomas, P. Doty, *J. Am. Chem. Soc.* **1954**, *76*, 3047–3053.
[52] J. D. McGhee, P. H. von Hippel, *J. Mol. Biol.* **1974**, *86*, 469–489.
[53] M. T. Carter, M. Rodriguez, A. J. Bard, *J. Am. Chem. Soc.* **1989**, *111*, 8901–8911.
[54] S. Saha, R. Majumdar, M. Roy, R. R. Dighe, A. R. Chakravarty, *Inorg. Chem.* **2009**, *48*, 2652–2663.
[55] J. Bernadou, G. Pratviel, F. Bennis, M. Girardet, B. Meunier, *Biochemistry* **1989**, *28*, 7268–7275.

Received: November 11, 2013
Published Online: ■



  

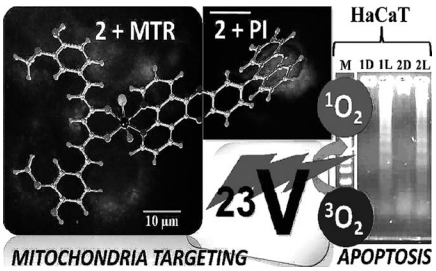


Dedicated Issue

  